URF PUBLISHERS
connect with research world

Journal of Cell Science and Regenerative Medicine

https://urfpublishers.com/journal/cell-science-regenerative-medicine

Volume 1, Issue 1 (Mar) 2025

Research Article

The Effect of Fullerene Derivatives with Two Different Types of Aromatic Addends on the Level of Oxidative Damage in HELF Cells

Tatyana A Salimova[1], Larisa V Kameneva[1], Elizaveta S. Ershova[1*], Valeriya S Bolshakova[2], Olga A Kraevaya[2], Alexander S Peregudov[3], Pavel A Troshin[2,4], Ekaterina A Savinova[1], Natalia N Veiko[1] and Svetlana V Kostyuk[1]

[1]Research Centre for Medical Genetics, ul. Moskvorechye 1, 115522 Moscow, Russia

[2]Federal Research Center of Problems of Chemical Physics and Medicinal Chemistry of the Russian Academy of Sciences, Semenov Prospect 1, Chernogolovka, 142432, Russia

[3]AN Nesmeyanov Institute of Organoelement Compounds of the Russian Academy of Sciences, Vavilov Str. 28, 119991 Moscow, Russia

[4]Zhengzhou Research Institute of HIT, 26 Longyuan East 7th, Jinshui District, Zhengzhou, Henan Province, 450000, China

Citation: Salimova TA, Kameneva LV, Ershova ES, et al., The Effect of Fullerene Derivatives with Two Different Types of Aromatic Addends on the Level of Oxidative Damage in HELF Cells. *J Cell Sci Regenerative Med 2025;* 1(1): 17-23.

Received: 17 February, 2025; **Accepted:** 28 February, 2025; **Published:** 03 March, 2025

***Corresponding author:** Elizaveta S. Ershova, 1Research Centre for Medical Genetics, ul. Moskvorechye 1, 115522 Moscow, Russia. Email: es-ershova@rambler.ru

Copyright: © 2025 Ershova ES, et al., This is an open-access article distributed under the terms of the Creative Commons Attribution License, which permits unrestricted use, distribution, and reproduction in any medium, provided the original author and source are credited.

ABSTRACT

The study investigated the effect of four fullerene derivatives with two different types of aromatic addends attached to the fullerene cage on the viability of cultured human embryonic lung fibroblasts to assess their biocompatibility as a criterion for potential application (HELF). These compounds are promising antiviral agents.

Methods: MTT test to determine the non-cytotoxic concentration range; Flow cytometry: The compounds under study were added to the HELF culture medium, incubated for 1 to 24 hours and the level of double-stranded DNA breaks, DNA oxidation, the level of reactive oxygen species and the levels of NRF2 and NOX4 proteins were studied using flow cytometry.

Results: All compounds exhibited a non-cytotoxic concentration range in the MTT assay. For fullerene derivatives with the first type of addends, treatment of HELFs (human embryonic lung fibroblasts) with the new water-soluble fullerene derivatives induced increased NOX4 levels. In F1-treated cells, this was accompanied by elevated NRF2 levels, while F2 treatment showed no such effect. Consequently, ROS levels in F1-treated cells remained below control values, whereas F2 treatment resulted in ROS levels exceeding the control by 24 hours.. he derivatives with the second type of substituents (F3 and F4) were characterized by substantially reduced ROS induction compared to the first group.

Conclusion: All compounds exhibited a non-cytotoxic concentration range in HELF cells, confirming their biocompatibility. A single compound was selected based on its ability to: avoid oxidative DNA damage and double-strand breaks and maintain intracellular ROS levels below control values for 24 hours.

Keywords: Fullerene Derivatives, Reactive Oxygen Species, Antioxidant Properties, Antiviral Activity, Genotoxicity

1. Introduction

Rapidly advancing nanotechnology is facilitating the production and application of numerous novel compounds, including water-soluble C_{60} fullerene derivatives, across diverse fields. Their potential medical applications are being investigated, including as antioxidants, neuroprotective agents and stimulators of antitumor immunity[1-7]. Fullerenes hold tremendous potential as alternatives to conventional chemotherapy or radiotherapy for tumor treatment[8-10]. In a substantial number of contemporary studies, fullerene derivatives are investigated as antiviral agents, with demonstrated efficacy against SARS-CoV-2, herpes simplex virus, cytomegalovirus, influenza virus, HIV, Ebola virus and other pathogens[11-18].

Several research groups have identified the ability of C_{60} and C_{70} fullerene derivatives to stabilize immune effector cells and consequently inhibit proinflammatory cytokine release. This property suggests their potential for developing pharmaceutical agents against various diseases, including asthma, arthritis and multiple sclerosis[19-22]. Nanoparticles have gained regulatory approval as delivery vehicles for targeted gene and antiviral drug transport[23-26].

When designing the synthesis of novel promising derivatives, it is essential to consider not only their target activity but also to evaluate their overall effects on cells and organisms[27-30]. These potential risks represent the most significant challenge in applying nano-compounds. Data on the effects of fullerene derivatives on cultured cells will help draw preliminary conclusions about the biosafety of the investigated compounds and assess their potential for medical applications. A common approach has been to investigate both cytotoxicity and biocompatibility of promising compounds using cultured cell models[31-33]. Various research groups are investigating parameters such as cytotoxicity, effects on cell proliferation, cellular oxidative stress levels and associated oxidative DNA damage. Such studies frequently reveal unexpected effects - for instance, colloidal nano-C_{60} suspension has been shown to influence lipid peroxidation[34] or induce synthesis of proinflammatory cytokines[35].

Thus, biocompatibility assessment represents an essential stage in contemporary nanodrug development across all therapeutic applications. Moreover, it provides crucial insights into the interaction mechanisms between nanomaterials and living cells/organisms.

In this work, we studied the effects of four fullerene derivatives with two distinct types of aromatic addends attached to the fullerene cage on the viability of human embryonic lung fibroblasts. These compounds represent promising antiviral agents, with one class of modified derivatives having demonstrated antiviral properties[36].

2. Materials and methods

2.1. Synthesis and characteristics of fullerene C (60) derivatives

Novel fullerene derivatives F1-F2 were synthesized using the approach developed recently by our group **(Figure 1)**[36]. The utilized strategy is based on the reaction of precursor compounds C60Ar5Cl with substituted alkylthiophene in the presence of water. Molecular structures and compositions of novel compounds F1e-F2e, F1-F2 were confirmed using 1H, 13C, 2D 1H–1H COSY, 1H–13C HSQC and 1H–13C HMBC NMR spectroscopy and MALDI mass spectrometry (Fig.S1-S22, ESI). (Suppl.)

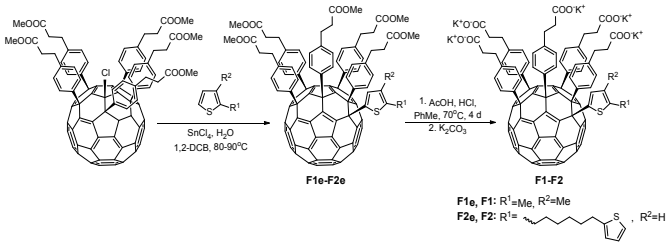

Figure 1: Synthesis of novel fullerene derivatives F1-F2.

Synthesis and characterization of compounds F3-F4 have been reported previously [37]. Both of them possessed significant antiviral activity (EC50 = 6.51.1± and 1.80.3± μM) against Influenza A/Puerto Rico/8/34 (H1N1) virus and low cytotoxicity (CC50>134 and 111 μM), which resulted in high selectivity indexes of >21 and 62 respectively.

The compounds are highly soluble in water and nutrient media.

2.2. Cell culture

The study was conducted using human embryonic lung fibroblasts (HFLF) from the RCMG cell culture collection, with approval from the RCMG Ethics Committee for Medical and Biological Research (Protocol No. 5). Cells were cultured in DMEM medium (Paneco, Moscow, Russia) supplemented with 10% fetal bovine serum (S181H, Biovest), 50 U/mL penicillin and 50 μg/mL streptomycin (Paneco, Moscow, Russia). All experiments were performed with cells at passage 4. Test compounds were dissolved in physiological saline and added to cells 24 hours after seeding.

2.3. MTT assay

The MTT assay was performed according to standard protocols [38-39]. Cells were cultured in 96-well plates (SPL Life Science Co., Ltd, South Korea) for 72 hours in the presence of test compounds. Cell viability was assessed using 3-(4,5-dimethylthiazol-2-yl)-2,5-diphenyltetrazolium bromide (MTT), with optical density measurements taken at 550 nm using an En Spire multimode plate reader (PerkinElmer, Inc., USA).

2.4. Fluorescence microscopy

Cells were seeded onto slide flasks (SPL Life Science Co., Ltd, South Korea), incubated for 24 hours with fullerene derivatives and analyzed using an Axio Scope A1 fluorescence microscope (Carl Zeiss, Oberkochen, Germany).

2.5. Flow cytometry

Cells were detached from the substrate, washed with 1% albumin in PBS solution, fixed with 3.7% formaldehyde for 10 min at 37°C, washed again and permeabilized in 90% methanol overnight at -20°C. Prior to antibody staining, cells were pelleted, washed twice with PBS containing 1% BSA, resuspended in PBS and incubated overnight at 4°C with fluorochrome-conjugated specific antibodies (1 μg/ml). After PBS washing, samples were analyzed using a Cytoflex S flow cytometer (Beckman Coulter Inc., USA). The following antibodies were used:PE-8OHdG (sc-393871 PE, Santa Cruz, Dallas, TX, USA), CY5.5-NOX4

(bs-1091r-cy5-5, Bioss Inc., Woburn, MA, USA) ; FITC-NRF2 pSer40 (bs2013, Bioss Inc.); PE-8OHdG (sc-393871 PE, Santa Cruz, Dallas, TX, USA) ; DyLight488-γH2AX (pSer139) (nb100-78356G Novus Bio, Saint Louis, CO, USA) ;. Flow cytometry data analysis was performed using Cyt Expert 2.4.028 software (Beckman Coulter Inc, USA).

2.6. Reactive oxygen species assays

ROS analysis was performed by flow cytometry. Detached cells were washed and resuspended in 10 μM H_2DCFHDA solution (in PBS; Molecular Probes/Invitrogen, Carlsbad, CA, USA), incubated for 15 minutes in the dark at 37°C, pelleted, washed and immediately analyzed on a Cytoflex S flow cytometer (Beckman Coulter Inc., USA) using the FITC fluorescence channel.

2.7. Statistical analysis

All experiments were performed in three independent trials with triplicate replicates per condition. Flow cytometry data analysis utilized median fluorescence intensity values. Histograms display mean values ± standard deviation (SD). Statistical significance was determined using the nonparametric Mann-Whitney U-test, with p-values < 0.005 considered statistically significant. Data analysis was performed using: Microsoft Excel (Microsoft Office, Redmond, WA, USA), Statistica 6.0 (Dell Technologies, Round Rock, TX, USA), Stat Graphics Centurion (Statgraphics Technologies, The Plains, VA, USA)

3. Results

3.1. Description of the compounds

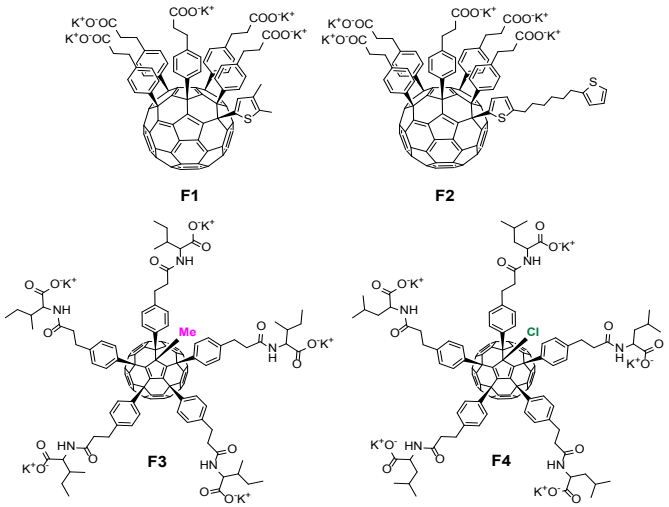

Figure 2: Molecular structures of water-soluble fullerene derivatives F1-F4.

Fullerene derivatives with two different types of aromatic addends attached to the fullerene cage have demonstrated promising antiviral activity against human immunodeficiency and influenza viruses.

Both of them (F3 and F4) possessed significant antiviral activity (EC50 = 6.51.1± and 1.80.3± μM) against Influenza A/ Puerto Rico/8/34 (H1N1)[37].

3.2. MTT assay

To evaluate the cytotoxicity of the test compounds against normal human cells (human embryonic lung fibroblasts, HELF), an MTT assay was performed across a concentration range of 4.2 ng/mL to 2.3 mg/mL.

Among the four tested compounds, F2 demonstrated the lowest cytotoxicity: in the concentration range of 4.2 ng/mL to 0.53 mg/mL, it showed no significant cytotoxic effects on HELF cells (inducing <10% cell death). However, at higher concentrations (≥2.3 mg/mL), F2 exhibited damaging effects, resulting in >30% HELF cell mortality **(Figure 3)**. The structurally similar compound F1 displayed a concentration-dependent biphasic effect - at 2.3 mg/mL it caused cell damage, which transitioned to stimulatory effects at intermediate concentrations, followed by renewed cytotoxic activity (10-20% cell death) at lower concentrations.

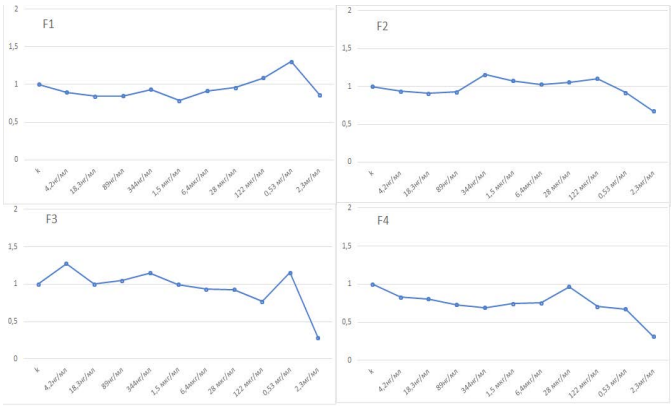

Figure 3: MTT assay: X-axis - fullerene concentrations (μg/mL); Y-axis - relative optical density at 550 nm.

Among the four tested compounds, F2 exhibited the lowest cytotoxicity. In the concentration range of 4.2 ng/mL to 0.53 mg/mL, F2 showed no significant cytotoxic effects on HELF cells (<10% cell mortality). However, at higher concentrations (≥2.3 mg/mL), it demonstrated damaging effects, resulting in >30% HELF cell death **(Figure 3)**. The structurally analogous compound F1 displayed a triphasic concentration-dependent response: cytotoxic effects at 2.3 mg/mL transitioned to stimulatory activity at intermediate concentrations, followed by renewed cytotoxicity (10-20% cell death) at lower concentrations. Compounds F3 and F4 - differing by Cl (F4) and Me (F3) substitutions - exhibited toxicity at concentrations ≥2.3 mg/mL. Between these structural analogs, F3 ceased its damaging effects upon concentration reduction, while F4 maintained persistent negative effects (albeit diminished) without reaching control levels. Notably, F3 demonstrated punctate proliferative enhancements at both 4.2 pg/mL and 0.5 mg/mL, while F4 showed similar effects at 28 μg/mL.

Based on MTT assay results for comparative biocompatibility assessment (evaluating fullerene effects on intracellular ROS levels, oxidative DNA damage and antioxidant response), we selected two non-cytotoxic concentrations: 10 nM and 15 μM.

3.3. Fluorescence analysis of water-soluble fullerene-based compounds in living cells

Most water-soluble fullerene derivatives we previously studied exhibit fluorescence in the red spectral region, enabling visualization of their cellular uptake and localization[38-41], as well as assessment of their internalization kinetics. All investigated compounds (F1-F4) enter the cytoplasm of individual HELF cells in the population and localize cytoplasmically without nuclear penetration.

Thus, all compounds exhibit characteristic fluorescence upon interaction with cells in culture medium, enabling investigation of their cellular uptake, cytoplasmic accumulation and subcellular localization **(Figure 4)**.

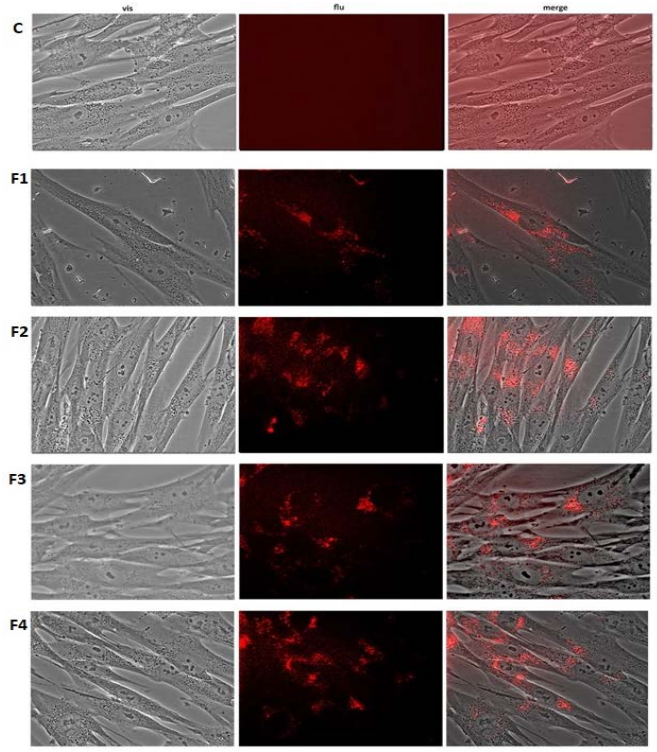

Figure 4: Fluorescence of LV-269 (A), LV-276 (B), LV-417 (C) and LV-416 (D) at 28 μg/mL in cells after 24-hour incubation. Merged bright-field and red-spectrum fluorescence images (100× magnification).

3.4. Effect of fullerene derivatives on oxidative DNA modifications and strand breaks in HELF cells

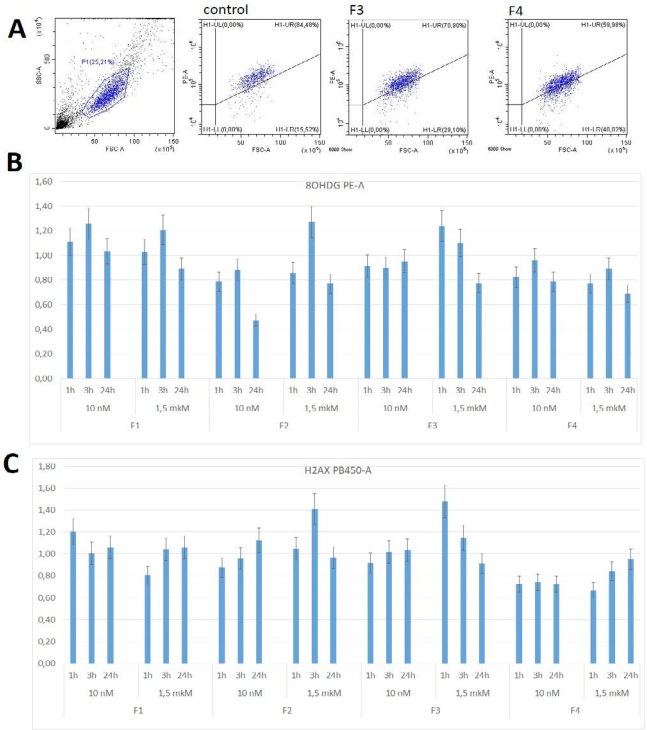

Figure 5: A - Cell distribution profiles of DNA oxidation marker -8oxodG following -24hour incubation with compounds F3 and F15(4 μM). Flow cytometry data. B - Histogram of -8OHdG levels for compounds F-1F4 (median fluorescence intensities normalized to untreated controls). C - Histogram of phosphorylated histone H2AX (γ-H2AX) levels in HELF cells. Incubation times and concentrations are indicated in the figure.

Nuclear DNA damage was assessed by quantifying two biomarkers: 8-hydroxy-2'-deoxyguanosine (8-oxodG) for oxidative base modifications and DNA double-strand breaks (DSBs)[42-45]. Treatment with compounds F1 and F2 (10 nM and 15 μM) initially reduced DNA oxidation levels, followed by an increase at 3 hours and subsequent reduction after 24 hours. For the second pair of compounds, F3 and F4, the effects differed: F3 at lower concentrations showed minimal impact on nuclear 8-OHdG levels in cellular DNA, while at 1.5 μM it caused a statistically significant increase that subsequently decreased below control levels after 3 and 24 hours. Compound F4 at concentrations of 10 nM and 1.5 μM reduced 8-oxodG levels below control values at all incubation timepoints **(Figure 5B)**.

DNA oxidation and subsequent elevation of 8-oxodG levels induce nuclear DNA strand breaks in cells (genotoxic effect). The level of nuclear DNA double-strand breaks (DSBs) was quantified by measuring phosphorylated histone H2AX (γ-H2AX), a conserved chromatin-associated protein. Phosphorylation at serine 139 occurs specifically at DSB sites during DNA damage response. The level of phosphorylated histone H2AX (γ-H2AX) generally correlates with 8-hydroxy-2'-deoxyguanosine (8-OHdG) content in DNA. Compound F1 exhibited both marginal increases and decreases in γ-H2AX levels. While F2 at 10 nM showed no significant effects, treatment with 1.5 μM for 3 hours resulted in elevated DNA double-strand breaks (paralleling the 8-oxodG increase). For compound F3 at 10 nM, the level of phosphorylated histone H2AX (γ-H2AX) remained at control levels. However, at 1.5 μM concentration: after 1 hour: γ-H2AX levels increased, after 3 hours levels decreased; after 24 hours: further reduction below control levels.

F4 reduced double-strand break (DSB) levels at all tested concentrations and incubation times, with the effect being most pronounced at 10 nM **(Figure 5C)**.

3.5. Analysis of reactive oxygen species (ROS) levels, the transcription factor NRF2 (responsible for the antioxidant response in cells) and NOX4

Oxidative DNA damage is directly linked to intracellular ROS levels. Many fullerene derivatives exhibit potent antioxidant properties in solution[45, 46]. However, the antioxidant mechanism of nano-compounds in living cells is more complex: Elevated ROS levels trigger cellular antioxidant defense mechanisms, primarily mediated by the transcription factor NRF2, which orchestrates the expression of protective antioxidant proteins to mitigate oxidative damage. Excessive ROS scavenging by nano-compounds or an overactive cellular antioxidant response may reduce ROS levels below physiologically required thresholds. This can trigger compensatory free radical production, potentially leading to paradoxical ROS elevation[46-48]. Such rebound effects may counteract the radical-binding capacity of fullerene derivatives.

NOX4, the predominant NADPH oxidase in fibroblasts, was investigated as the key physiological ROS source in this study **(Figure 6).**

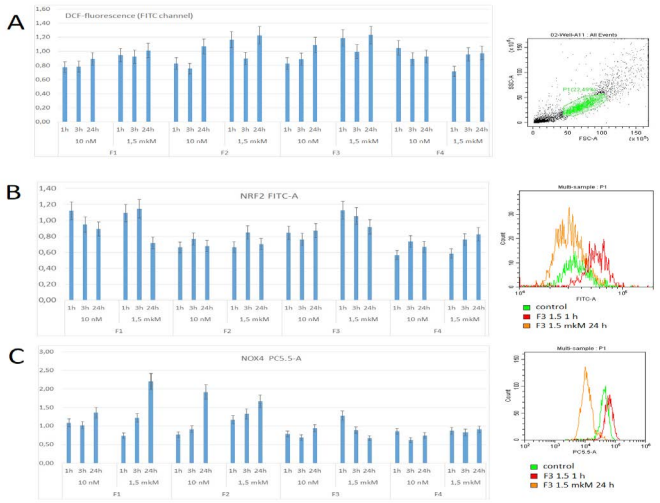

Figure 6: Flow Cytometry Data. A - Reactive oxygen species (ROS) levels (DCF fluorescence signal measurement). Dot plot shows gated cell population used for signal quantification. B - NRF2 levels histogram for compounds F1-F4. Representative cell distribution by fluorescence signal (NRF2-FITC) - F3 treatment at 1.5 μM, 1-hour and 24-hour incubations. C - NOX4 levels histogram in HELF cells. Representative fluorescence signal distribution (NOX4-Cy5.5) - F3 treatment at 1.5 μM, 1-hour and 24-hour incubations. All incubation times and concentrations are indicated in the figure. Signals were normalized to control (untreated cells).

Intracellular ROS levels were measured using H_2DCFH-DA (2',7'-dichlorodihydrofluorescein diacetate). The hydrolyzed intracellular product DCFH serves as a sensitive oxidative stress marker, undergoing ROS-dependent oxidation to highly fluorescent DCF. Fluorescence was quantified by flow cytometry (FITC channel). Figure 6 presents the ratios of median DCF fluorescence intensities in cells treated with fullerene derivatives (10 nM and 15 μM) relative to untreated controls across different incubation periods (1, 3 and 24 hours). Compounds F2 and F3 exhibit antioxidant properties at 10 nM, while F1 and F4 reduce ROS levels in HELF cells at both tested concentrations (10 nM and 15 μM). However, by 24 hours, all treatments show partial ROS rebound, remaining below control levels.

The observed cytoprotection arises through three synergistic mechanisms: (i) direct radical neutralization by fullerene cores, (ii) suppression of NOX4-derived superoxide generation and (iii) NRF2-dependent upregulation of phase II detoxification enzymes. When analyzing the level of NRF2 and NOX4 proteins for compound F1, activation of the transcription factor NRF2 is observed at an incubation time of 1 hour for a concentration of 1 nM and 1 and 3 hours for a concentration of 1.5 μM; by 24 hours of incubation, the amount of NRF2 decreases and the level of NOX4 increases 2-fold relative to the control, which is consistent with the onset of an increase in ROS.

In the case of F2, the level of NRF2 is lower than the control and NOX4 increases with incubation time, for a low concentration by 24 hours it exceeds the control and for a higher concentration it increases almost 1.8 times relative to the control. A common feature of compounds of the same type F1 and F2 is an increase in the level of NOX4 depending on the incubation time of the compounds with cells.

For F3, at a concentration of 10 nM, we do not observe activation of transcriptional NRF2 and NOX4 is below the control level - and the ROS level is also below the control; at a concentration of 1.5 μM with an incubation time of 1 hour, the ROS level is elevated, there is a slight increase in NRF2 and NOX4, then by 3 hours the levels of NRF2, NOX4 and ROS return to the control and by 24 hours NRF2, NOX4 are further reduced, but ROS in the cells increases.

Cells incubated with F4 for 24 h have a slightly reduced level of ROS, but do not show activation of either NOX4 or NRF2.

A common feature of F3 and F4 derivatives, which distinguishes them from F1-2, is a lower stimulation of ROS synthesis.

4. Discussion and Conclusion

For each of the 4 compounds, a significant concentration range was found in which the compound did not exert a cytotoxic effect on HELF, thus all compounds are biocompatible. Further analysis of the effect of genotoxicity of fullerene derivatives and their antioxidant properties on HELF revealed group and individual differences. Since the action of new water-soluble derivatives of fullerenes F1 F2 on FLECH leads to an increase in the level of NOX4, for F1 it is accompanied by an increase in the level of NRF2, but for F2 this is not observed. As a result, the level of ROS in cells incubated with F1 is lower than the control and for F2 it exceeds the control by 24, but even a short-term increase in the level of active free radicals can damage the DNA of cells - and here we observe an increased level of 8-oxodG during incubation for 3 hours.

Compound F3 at 10 nM concentration demonstrates no genotoxic effects. However, at 1.5 μM concentration, it induces both double-strand breaks and DNA oxidation within short-term exposure (1-3 hours).

The most notable is compound F4, which induces neither oxidative DNA damage nor double-strand breaks. It maintains intracellular ROS levels below control values for 24 hours and does not activate NOX4 (thus avoiding ROS synthesis induction) during incubation.

5. Acknowledgement

The contribution of Center for molecule composition studies of INEOS RAS is gratefully acknowledged.

6. Conflict of Interest

The authors declare no conflict of interest.

7. Funding

The study was supported by a government assignment from the Ministry of Science and Higher Education.

8. Supplementary Materials

The following supporting information can be downloaded Molecular structures and compositions of novel compounds F1e-F2e, F1-F2 were confirmed using ^{1}H, ^{13}C, 2D ^{1}H-^{1}H COSY, ^{1}H-^{13}C HSQC and ^{1}H-^{13}C HMBC NMR spectroscopy and MALDI mass spectrometry (Fig.S1-S22, ESI).

9. Author Contributions

Conceptualization, E.S.E. and S.V.K.; methodology, S.V.K., E.S.E. and N.N.V validation, S.V.K., E.S.E. and P.A.T.; investigation, T.A.S. E.A.S., L.V.K., V.S.B. O.A.K and E.S.E.;

resources, S.V.K., N.N.V., P.A.T. and A.S.P.; data curation, S.V.K., P.A.T. and N.N.V.; writing-original draft preparation, E.S.E. and T.A.S.; writing-review and editing, S.V.K. and E.S.E..; visualization, N.N.V supervision, S.V.K. and N.N.V.; project administration, A.S.P., S.V.K., P.A.T. funding acquisition, S.V.K., P.A.T. All authors have read and agreed to the published version of the manuscript.

10. Data Availability Statement

The datasets used and/or analyzed during the current study are available from the corresponding author on reasonable request.

11. References

1. Sridharan R, Monisha B, Kumar PS, et al. Carbon nanomaterials and its applications in pharmaceuticals: A brief review. Chemosphere, 2022;294: 133731.
2. Mashino T. Development of Bio-active Fullerene Derivatives Suitable for Drug. Yakugaku Zasshi, 2022;142: 165-179.
3. Hou W, Shen L, Zhu Y, et al. Fullerene Derivatives for Tumor Treatment: Mechanisms and Application. Int J Nanomedicine, 2024;19: 9771-9797.
4. Li L, Zhen M, Wang H, et al. Functional Gadofullerene Nanoparticles Trigger Robust Cancer Immunotherapy Based on Rebuilding an Immunosuppressive Tumor Microenvironment. Nano Lett, 2020;20: 4487-4496.
5. Norton SK, Wijesinghe DS, Dellinger A, et al. Epoxyeicosatrienoic acids are involved in the C70 fullerene derivative–induced control of allergic asthma. J Allergy Clin Immunol, 2012;130: 761-769.
6. Zhou Z, Lenk RP, Dellinger A, et al. Liposomal Formulation of Amphiphilic Fullerene Antioxidants. Bioconjugate Chem, 2010;21: 1656-1661.
7. Oh H, Lee JS, Son P, et al. Highly Water-Dispersed Natural Fullerenes Coated with Pluronic Polymers as Novel Nano antioxidants for Enhanced Antioxidant Activity. Antioxidants (Basel), 2024;13: 1240.
8. Hou W, Shen L, Zhu Y, et al. Fullerene Derivatives for Tumor Treatment: Mechanisms and Application. Int J Nanomedicine, 2024;19: 9771-9797.
9. Sharma DK. Recent advancements in nanoparticles for cancer treatment. Med Oncol, 2025;42: 72.
10. Li Y, Xu Z, Qi Z, et al. Application of Carbon Nanomaterials to Enhancing Tumor Immunotherapy: Current Advances and Prospects. Int J Nanomedicine, 2024;19: 10899-10915.
11. Katin KP, Kochaev AI, Kaya S, et al. Ab Initio Insight into the Interaction of Metal-Decorated Fluorinated Carbon Fullerenes with Anti-COVID Drugs. Int J Mol Sci, 2022;23: 2345.
12. Kraevaya OA, Bolshakova VS, Slita AV, et al. Buckyballs to fight pandemic: Water-soluble fullerene derivatives with pendant carboxylic groups emerge as a new family of promising SARS-CoV-2 inhibitors. Bioorg Chem, 2025;154: 108097.
13. Mashino T, Shimotohno K, Ikegami N, et al. Human immunodeficiency virus-reverse transcriptase inhibition and hepatitis C virus RNA-dependent RNA polymerase inhibition activities of fullerene derivatives. Bio org Med Chem Lett, 2005;15: 1107-1109.
14. Tollas S, Bereczki I, Borbás A, et al. Synthesis of a cluster-forming sialylthio-d-galactose fullerene conjugate and evaluation of its interaction with influenza virus hemagglutinin and neuraminidase. Bio org Med Chem Lett, 2014;24: 2420-2423.
15. Muñoz A, Sigwalt D, Illescas BM, et al. Synthesis of giant globular multivalent glycofullerenes as potent inhibitors in a model of Ebola virus infection. Nat Chem, 2016;8: 50-57.
16. Sinegubova EO, Kraevaya OA, Volobueva AS, et al. Water-soluble fullerene C60 derivatives are effective inhibitors of influenza virus reproduction, Microorganisms, 2023;11: 681.
17. Sengupta J, Hussain CM. The Emergence of Carbon Nanomaterials as Effective Nano-Avenues to Fight against COVID-19. Materials (Basel), 2023;16: 1068.
18. Panda M, Purohit P, Wang Y, et al. Functionalized carbon nanotubes as an alternative to traditional anti-HIV-1 protease inhibitors: An understanding towards Nano-medicine development through MD simulations. J Mol Graph Model, 2022;117: 108280.
19. Norton SK, Wijesinghe DS, Dellinger A, et al. Epoxyeicosatrienoic acids are involved in the C (70) fullerene derivative-induced control of allergic asthma. J Allergy Clin Immunol, 2012;130: 761-769.
20. Zhou Z, Lenk RP, Dellinger A, et al. Liposomal formulation of amphiphilic fullerene antioxidants. Bioconjug Chem, 2010;21: 1656-1661.
21. Basso AS, Frenkel D, Quintana FJ, et al. Reversal of axonal loss and disability in a mouse model of progressive multiple sclerosis. J Clin Invest, 2008;118: 1532-1543.
22. Ambesh P, Angeli DG. Nanotechnology in neurology: Genesis, current status and future prospects. Ann Indian Acad Neurol, 2015;18: 382-386.
23. Sigwalt D, Holler M, Iehl J, et al. Gene delivery with polycationic fullerene hexakis-adducts. Chem Commun (Camb), 2011;47: 4640-4642.
24. Fan J, Fang G, Zeng F, et al. Water-dispersible fullerene aggregates as a targeted anticancer prodrug with both chemo- and photodynamic therapeutic actions. Small, 2013;9: 613-621.
25. Yao C, Xiang F, Xu Z. Metal oxide nanocage as drug delivery systems for Favipiravir, as an effective drug for the treatment of COVID-19: a computational study. J Mol Model, 2022;28: 64.
26. Sengupta J, Hussain CM. The Emergence of Carbon Nanomaterials as Effective Nano-Avenues to Fight against COVID-19. Materials (Basel), 2023;16: 1068.
27. Ruan H, Zhang X, Yuan J, et al. Effect of water-soluble fullerenes on macrophage surface ultrastructure revealed by scanning ion conductance microscopy. RSC Adv, 2022;12: 22197-22201.
28. Fiorito S, Serafino A andreola F, Togna A, et al. Toxicity and biocompatibility of carbon nanoparticles. J Nanosci Nanotechnol, 2006;6: 591-599.
29. Stern ST, McNeil SE. Nanotechnology safety concerns revisited. Toxicol Sci, 2008;101: 4-21.
30. Lehto M, Karilainen T, Róg T, et al. Co-exposure with fullerene may strengthen health effects of organic industrial chemicals. PLoS One, 2014;9: 114490.
31. Zečević S, Popović D, Tomić S, et al. Anti-Inflammatory and Immunomodulatory Properties of Inorganic Fullerene-Like Tungsten Disulfide Nanoparticles in the Culture of Human Peripheral Blood Mononuclear Cells. Nanomaterials (Basel), 2025;15: 322.
32. Misra C, Kaur J, Kumar M, et al. Docetaxel-tethered di-Carboxylic Acid Derivatised Fullerenes: A Promising Drug Delivery Approach for Breast Cancer. AAPS Pharm Sci Tech, 2024;25: 233.
33. Lehto M, Karilainen T, Róg T, et al. Co-exposure with fullerene may strengthen health effects of organic industrial chemicals. PLoS One, 2014;9: 114490.
34. Sayes CM, Gobin AM, Ausman KD, et al. Nano-C60 cytotoxicity is due to lipid peroxidation. Biomaterials, 2005;26: 7587-7595.

35. Park EJ, Kim H, Kim Y, et al. Carbon fullerenes (C60s) can induce inflammatory responses in the lung of mice. Toxicol Appl Pharmacol, 2010;244: 226-233.

36. Bolshakova VS, Sinegubova EO, Esaulkova YL, et al. Facile Synthesis of Amino Acid Decorated Water-Soluble Fullerene Derivatives with Anti-influenza Activity Chin J Chem, 2023;41: 1803-1808.

37. Kraevaya OA, Bolshakova VS, Peregudov AS, et al. Water-Promoted Reaction of C60Ar5Cl Compounds with Thiophenes Delivers a Family of Multifunctional Fullerene Derivatives with Selective Antiviral Properties. Org Lett, 2021;23: 7226-7230.

38. Ershova ES, Sergeeva VA, Tabakov VJ, et al. Functionalized fullerene increases NF-kappa B activity and blocks genotoxic effect of oxidative stress in serum-starving human embryo lung diploid fibroblasts. Oxid Med Cell Longev, 2016;2016: 9895245.

39. Ershova ES, Sergeeva V, Chausheva AI, et al. Toxic and DNA damaging effects of a functionalized fullerene in human embryonic lung fibroblasts. Mutat Res Genet Toxicol Environ Mutagenesis, 2016;805: 46-57.

40. Kostyuk SV, Proskurnina EV, Savinova EA, et al. Effects of Functionalized Fullerenes on ROS Homeostasis Determine Their Cytoprotective or Cytotoxic Properties. Nanomaterials (Basel), 2020;10: 1405.

41. Sergeeva V, Kraevaya O, Ershova E, et al. Kostyuk Antioxidant Properties of Fullerene Derivatives Depend on Their Chemical Structure: A Study of Two Fullerene Derivatives on HELFs. Oxid Med Cell Longev, 2019: 4398695.

42. Winterbourn CC. Reconciling the Chemistry and Biology of Reactive Oxygen Species. Nat Chem Biol, 2008;4: 278-286.

43. Sies H, Jones DP. Reactive Oxygen Species (ROS) as Pleiotropic Physiological Signaling Agents. Nat Rev Mol Cell Biol, 2020;21: 363-383.

44. Ershova ES, Sergeeva VA, Chausheva AI, et al. Toxic and DNA damaging effects of a functionalized fullerene in human embryonic lung fibroblasts. Mutat Res Genet Toxicol Environ Mutagen, 2016;805: 46-57.

45. Ershova ES, Sergeeva VA, Tabakov VJ, et al. Functionalized Fullerene Increases NF-κB Activity and Blocks Genotoxic Effect of Oxidative Stress in Serum-Starving Human Embryo Lung Diploid Fibroblasts. Oxid Med Cell Longev, 2016;2016: 9895245.

46. Winterbourn CC. Reconciling the Chemistry and Biology of Reactive Oxygen Species. Nat Chem Biol, 2008;4: 278-286.

47. Sies H, Jones DP. Reactive Oxygen Species (ROS) as Pleiotropic Physiological Signaling Agents. Nat Rev Mol Cell Biol, 2020;21: 363-383.

48. Dinkova-Kostova AT, Copple IM. Advances and challenges in therapeutic targeting of NRF2. Trends Pharmacol Sci, 2023;44: 137-149.